Inertio Gravity Waves in the Upper Mesosphere

H. G. Mayr, J. G. Mengel., E. L. Talaat, H. S. Porter, K. L. Chan
[1]Goddard Space Flight Center, Greenbelt, MD, 20771
[2]Science Systems & Applications, Inc., Lanham, MD
[3]Applied Physic Laboratory, Johns Hopkins University, Laurel, MD
[4]Furman University, Greenville, SC
[5]Hong Kong University of Science and Technology, Hong Kong, China

Prepared for Submission

To

Geophysical Research Letters

June, 2003

Abstract: In the polar region of the upper mesosphere, horizontal wind oscillations have been observed with periods around 10 hours (Hernandez et al., 1992). Such waves are generated in our Numerical Spectral Model (NSM) and appear to be inertio gravity waves (IGW). Like the planetary waves (PW) in the model, the IGWs are generated by instabilities that arise in the mean zonal circulation. In addition to stationary waves for m = 0, eastward and westward propagating waves for m = 1 to 4 appear above 70 km that grow in magnitude up to about 110 km, having periods between 9 and 11 hours. The m = 1 westward propagating IGWs have the largest amplitudes, which can reach at the poles 30 m/s. Like PWs, the IGWs are intermittent but reveal systematic seasonal variations, with the largest amplitudes occurring generally in winter and spring. The IGWs propagate upward with a vertical wavelength of about 20 km.

I. Introduction

Hernandez et al. (1992a) reported evidence for the existence of a pronounced westward propagating wave with a period of 10.1 hours in the southern hemisphere near the pole. The data for this analysis were based on optical measurements derived from Doppler shifting and broadening of OH emissions at altitudes near 90 km, which yielded winds and temperatures respectively. Medium frequency radar measurements from the Scott Base at 78° S (Fraser, 1984, 1989) provided additional observations of horizontal winds. The measurements were carried out during austral winter in August 1991.

During the period of observations and at both stations, the 10-hour wave was apparent in the wind data. In the optical measurements, the wave dominated at the South Pole where a wind amplitude of 8 m/s was inferred at the 95% significance level. The wave was also seen with the radar at 78° S, but the semi-diurnal tide dominated there.

For geometric reasons, a horizontal wind oscillation at the pole must have zonal wave number m = 1, and the observed phase progression revealed that the wave was propagating westward. The related temperature variations for this wave number on the other hand must vanish at the pole, and the analysis by Hernandez et al. (1992a) indeed showed that for the periodicity they observed in the winds.

Hernandez et al. (1993) subsequently observed the 10-hour wave also during the southern winter of 1992 in the Antarctic polar region, but in this case it was accompanied by a westward propagating 12-hour wave of comparable magnitude they called an inertio gravity wave. Forbes et al. (1995) also observed the westward propagating 12-hour wave in the radar measurements

near the north pole and identified it as a non-migrating semi-diurnal tide. They suggested that this tide is the product of nonlinear interactions between the solar driven migrating semidiurnal tide and stationary planetary waves with wave number m = 1.

The above mechanism proposed by Forbes et al. (1995) does generate in our model the non-migrating semi-diurnal tide (Mayr et al., 2003). In the present paper we demonstrate that the model also generates in the polar region significant planetary wave oscillations with periods around 10 hours observed by Hernandez et al. (1992a, 1993).

II. Numerical Spectral Model

The Numerical Spectral Model (NSM) was introduced by Chan et al. (1994), and 2D as well as 3D applications were discussed to describe the wave driven equatorial oscillations (QBO and SAO) and the tides and planetary waves in the middle atmosphere (e.g., Mengel et al., 1994, 1998, 2001). More recently, the NSM was also applied to describe the non-migrating tides that are generated in the middle atmosphere with planetary waves (Mayr et al., 2003). In the NSM, presently, the planetary waves are solely excited by instabilities and then amplified by GW interactions (Mayr et al., 2001).

An integral part of the NSM is that it incorporates the Doppler Spread Parameterization (DSP) for small-scale GWs, formulated by Hines (1997, a, b). The DSP deals with a spectrum of waves that interact with each other to produce Doppler spreading, which in turn affects the interaction of the waves with the background flow.

The 3D version of the NSM discussed here mainly differs from earlier applications published in the literature in that we incorporate tropospheric heating for the zonal mean (m = 0) to reproduce qualitatively the observed zonal jets and temperature variations near the tropopause. Such a heat source we had earlier applied in our 2D model to study its effect on the QBO, and we find that it affects also the planetary waves significantly.

III. Model Results

With Figure 1a we show a contour plot of computed meridional winds for zonal wave number m = 1 at 84° N (Gaussian point) at altitudes between 70 and 110 km, covering a time span of 5 days in March of the third model year. This time span was selected as an example to reveal a wave pattern with evident periodicity close to 10 hours. The waves propagate upward with vertical wavelengths between 15 and 20 km, and their amplitudes are generally well above

10 m/s, growing with height. Shown in Figure 1b is a power spectrum of the m = 1 westward propagating waves at the same latitude, which is derived from a 20 day time span during the month of March as in Figure 1a. The 10-hour wave clearly stands out, and in this case it is stronger than the non-migrating semi-diurnal tide. This is an atypical result, but it reproduces the observations of Hernandez et al. (1992a) who also found the semi-diurnal tide to be weaker.

With Figure 2 we present for wave numbers m = 0 to 2 the maximum amplitudes of the stationary wave (a) and the eastward (b, c) and westward (d, e) propagating waves of the meridional winds with periods between 9 and 10.5 hours derived for a running window of 15 days within the time span 26 to 29 months. This shows that the 10-hour wave so prominent in Figure 1 is not unique. Waves with periods below 12 hours are generated in our model also for m = 0 and 2, and for m = 3 and 4 as well (not shown). Both eastward and westward propagating waves are produced. For the time span analyzed and the range of wave periods (9 to 10.5 hours), the m = 1 westward propagating component is largest with a peak of 25 m/s near 100 km. Unique for this wave number m = 1, the amplitudes do not vanish at the poles but can peak there. As seen from Figure 2, for the three wave numbers on display, the largest waves are generated in the northern hemisphere during the late winter months close to spring, which appears to be the prevailing trend in the seasonal variations.

To provide more details about the waves discussed, we present in Figure 3 contour plots of the amplitude spectra as functions of latitude, displayed at 100 km for wave numbers m = 1 and 2. For m = 1 (Figure 3a), the non-migrating semi-diurnal tide is prominent (39 m/s maximum) in both hemispheres during this time span from 26 to 29 months. By comparison, the 10-hour wave is weaker but still significant with 24 m/s at 84° latitude. A wave with period near 9 hours is also generated, and its amplitude peaks at 14 m/s. The latitude dependence of these two waves suggest that they grow in magnitude to reach still larger values at the north pole. A weaker eastward propagating wave (dotted lines) is generated (Figure 3a), with maximum amplitude of about 10 m/s, but apparently it does not extend into the polar region.

For m = 2, we show in Figure 3b the large westward migrating semi-diurnal tide, which has a peak close to 50 m/s that is not resolved with the chosen contour interval of 1 m/s. In addition to that, in the northern hemisphere, a distinct westward propagating wave appears with period close to 10 hours, and two eastward propagating waves of similar magnitudes appear that have periods close to 9 and 11 hours.

A limited survey of the results from our model reveals that curious situations can develop not unlike that presented in Figure 1, where the 10-hour wave near the pole has larger amplitudes than the non-migrating semi-diurnal tide as Hernandez et al. had observed. A similar situation (not shown) we also encounter for m = 1 in the southern hemisphere during September of the third model year. During this month, a pronounced 9-hour wave appears with 26 m/s amplitude, and in this case again the non-migrating semi-diurnal tide near the south pole is weaker at 14 m/s. We also note that in m = 2, during the same season, a pronounced 11 m/s wave is generated in the southern hemisphere, which has a period close to 9.5 hours.

That the waves discussed reveal systematic seasonal variations is shown more explicitly in Figure 4. Here we present for m = 1 at 100 km the eastward (a) and westward (b) propagating waves in the meridional winds displayed as contour plots versus latitude and time covering 24 months. The maximum values (15.6 m/s, eastward; 26. 8 m/s, westward) and the minimum contours (1.5 m/s eastward; 5 m/s, westward) are stated. In both hemispheres, both wave components tend to be excited preferentially during winter months, beginning in late fall and extending into spring. Consistent with the results shown earlier, the westward propagating waves for this wave number are largely confined to high latitudes. The eastward propagating waves in contrast do not appear to extend into the polar regions but instead extend to low latitudes and across the equator. To some extent, the wave patterns for m = 2 (not presented) show similar trends, except that the winds for this (and all other wave numbers except m = 1) vanish at the poles.

To reveal the nature of the waves, we present in Figure 5 contour plots of snap-shots for the eastward (a) and westward (b) propagating components. The meridional winds were derived for a short time span near 32.5 months. This shows that the horizontal wavelength is about 40° and that the latitudinal variations for the eastward and westward propagating waves differ significantly as seen in Figure 4. The vertical wavelength is about 20 km, which was apparent also from Figure 1.

IV. Discussion and Conclusion

The above discussed waves appear to be related to the normal modes of Class I discussed by Longuett Higgins (1973), which are also referred to as global-scale Gravity Waves or Inertio Gravity Waves (Volland, 1988; Andrews, Holton, and Leovy, 1990). Unlike Rossby waves, Inertio Gravity Waves (IGW) have short enough periods so that the Coriolis force cannot

dominate over the inertial acceleration. Yet the periods are long enough so that the Coriolis force is still important. Under this condition, it is reasonable to expect that the eastward and westward propagating components differ significantly. For m = 1, the Class I waves in Longuett Higgins (1973) show the westward components to peak at the poles, while the eastward components tend to peak at mid latitudes. This is qualitatively consistent with the numerical results we presented. The latitudinal structure of the prominent waves we discussed have horizontal wavelengths of about 40°, which suggests that they are related to Class I modes of order 9 in the notation of Longuett Higgins (1973). And the periods associated with these wave modes are in the range generated in the model.

Considering that the waves in our model have vertical wave lengths of about 20 km (Figures 1 and 5), our conclusion differs from that reached by Hernandez et al. (1992a) who inferred a much larger wave length more commensurate with Lamb Waves.

Referring to the observations by Hernandez et al. (1992a), Forbes et al., (1995) argued that they likely represent a 12-hour non-migrating tide generated by stationary planetary waves interacting with the migrating tide. Forbes et al. had convincing observational evidence for strong non-migrating tides in the polar region, but their argument against the 10-hour wave in part relied on the assumption that other normal modes had not been observed - and it still needs to be seen whether such modes can be observed.

As mentioned earlier, we have been able to show that the mechanism proposed by Forbes et al. does generate the non-migrating tides in our model. But the 10-hour wave observed by Hernandez et al. may also be real. Such waves clearly develop in our model, and they are distinctly different from the non-migrating tides. For m = 1, the waves generated in the polar region have periods between 9 and 11 hours, and they are accompanied by waves with similar periods at other wave numbers as well, both eastward and westward propagating. We have also shown that these waves, identified as Inertio Gravity Waves, can be relatively strong in the polar regions during times (seasons) when the nonmigrating semidiurnal tides are weak as Hernandez et al. (1992a) observed.

References

Andrews, D. G., J. R. Holton, and C. B. Leovy, *Middle Atmosphere Dynamics*, Academic Press, Orlando, 1987.

Chan, K. L., H. G. Mayr, J. G. Mengel, and I. Harris, A 'stratified' spectral model for stable and convective atmospheres, *J. Comp. Phys.*, **113**, 165, 1994.

Chan, K. L., H. G. Mayr, J. G. Mengel, and I. Harris, A spectral approach for studying middle and upper atmospheric phenomena, *J. Atmos. Terr. Phys.*, **56**, 1399, 1994.

Forbes, J. M., and H. B. Garrett, Thermal excitation of atmospheric tides due to insolation absorption by O_3 and H_2O, *Geophys. Res. Lett.*, **5**, 1013, 1978.

Forbes, J. M., N. A. Makarov, Y. I. Portnyagin, First results from the meteor radar at South Pole: A large 12-hour oscillation with zonal wavenumber one, *Geophys. Res. Lett.*, **22**, 3247, 1995.

Fraser, G. J., Summer circulation in the Antarctic middle atmosphere, *J. Atm. Terr. Phys.*, **46**, 143, 1984

Fraser, G. J., Monthly mean winds in the mesosphere at 44°S and 78°S, *Pure Appl. Geophys.* **130**, 291, 1989.

Hernandez, G., R. W. Fraser, and Smith, G. J., Mesospheric 12-hour oscillation near south pole antarctica, *Gephys. Res. Lett.*, **20**, 1787, 1993.

Hernandez, G., R. W. Smith, G. J. Fraser, and W. L. Jones, Large-scale waves in the upper mesosphere at antarctic high-latitudes, *Gephys. Res. Lett.*, **19**, 1347, 1992a.

Hernandez, G., R. W. Smith, G. J. Fraser, and W. L. Jones, Neutral wind and temperature in the upper mesosphere above South Pole, *Gephys. Res. Lett.*, **19**, 53, 1992b.

Hines, C. O., Doppler-spread parameterization of gravity-wave momentum deposition in the middle atmosphere, 1, Basic formulation, *J. Atmos. Solar Terr. Phys.*, **59**, 371, 1997a.

Hines, C. O., Doppler-spread parameterization of gravity-wave momentum deposition in the middle atmosphere, 2, Broad and quasi monochromatic spectra, and implementation, *J. Atmos. Solar Terr. Phys.*, **59**, 387, 1997b.

Longuett-Higgins, M. S., The eigenfunctions of Laplace's tidal equations over a sphere, *Phi. Trans. Roy. Soc. London*, **A262**, 511, 1968.

Mayr, H. G., J. G. Mengel, E., R. Talaat, H. S. Porter, and K. L. Chan, Non-migrating tides, with zonally symmetric component, generated in the mesosphere, Paper EAE03-A-03691, presented at EGS-AGU-EUG Joint Assembly, Nice, France, 2003.

Mayr, H. G., J. G. Mengel, K. L. Chan, and H. S. Porter, Mesosphere dynamics with gravity forcing: Part II, Planetary waves, *J. Atm. Solar-Terr. Phys.*, **63**, 1865, 2001.

Mayr, H. G., J. G. Mengel, K. L. Chan, and H. S. Porter, Seasonal variations of the diurnal tide induced by gravity wave filtering, *Geophys. Res. Lett.*, **25**, 943, 1998.

Mengel, J. G., Mayr, H. G., Chan, K. L., Hines, C. O., Reddy, C. A., Arnold, N. F., Porter, H. S., Equatorial oscillations in the middle atmosphere generated by small-scale gravity waves, *Geophys. Res. Lett.*, **22** , 3027, 1995.

Strobel, D. F., Parameterization of atmospheric heating rate from 15 to 120 km due to O2 and O3 absorption of solar radiation, *J. Geophys. Res.*, **83**, 7963, 1978.

Volland, H., *Atmospheric Tidal and Planetary Waves*, Kluwer Academic Publ., Boston, MA, 1988.

Figure Captions

Figure 1: Contour plot of meridional winds (a) for zonal wave number m = 1 at 84° N and 100 km altitude during the month of March in the second model year (26 to 27 months) when the 10-hour wave happened to dominate at polar latitudes. For a running window of 20 days, the power spectrum of the westward propagating waves is shown during this time span (b), which reveals maximum wind amplitude of about 20 m/s that is larger in magnitude than that of the non-migrating 12-hour tide in this case. This model simulation thus mimics the situation encountered in the wind observations of Hernandez et al. (1992a) during the austral winter of 1991 in the southern hemisphere.

Figure 2: Maximum meridional wind amplitudes of the stationary m = 0 wave (a), and the eastward (b, c) and westward (d, e) propagating waves (m = 1, 2) for periods from 9 to 10.5 hours computed with a running window of 15 days from the time span between 26 and 29 months. Contour plots are presented versus height and latitude, applying the Mercator transformation to expand the regions at high latitudes where the waves are most prominent. The lowest 30% of contours are suppressed to eliminate cluttering, and the maximum amplitudes are recorded in each panel.

Figure 3: Maximum amplitude spectra for zonal wave numbers m = 1 (a) and 2 (b) at 100 km for periods between 8 and 14 hours computed from the 26 to 29 months time span with a running window of 15 days. Solid and dotted contours describe respectively the westward eastward propagating components. Note the non-migrating semi-diurnal tides (12 hour period) at m = 1 that peak at the poles (a), which are produced in the NSM (Mayr et al., 2003) through non-linear interaction between the solar driven migrating tide and stationary m = 1 planetary waves as Forbes et al. (1995) had proposed. The x-marks on the vertical axes denote the periods sampled to produce the contours.

Figure 4: Seasonal and latitudinal variations of the eastward (a) and westward (b) m = 1 waves in the meridional winds with periods between 9 and 10.5 hours at 100 km computed over a time span of 24 months. Stated are the values of maximum amplitudes and minimum contours. In contrast to the westward waves that tend to peak at the poles, the eastward waves do not extend with significant amplitudes into the polar regions but instead extend with larger amplitudes towards lower latitudes. The largest amplitudes for both components occur preferentially during winter months. The seasonal variations for the m = 2 waves (not shown) reveal similar trends except that they completely vanish at the poles.

Figure 5: Snap-shots of contour plots for the time of 32.5 months (late southern winter) when the waves are prominent. The characteristic differences between the eastward and westward propagating components are evident, each revealing a horizontal wavelength of about 40° latitude. As seen already from Figure 1, the vertical wavelength is about 20 km.

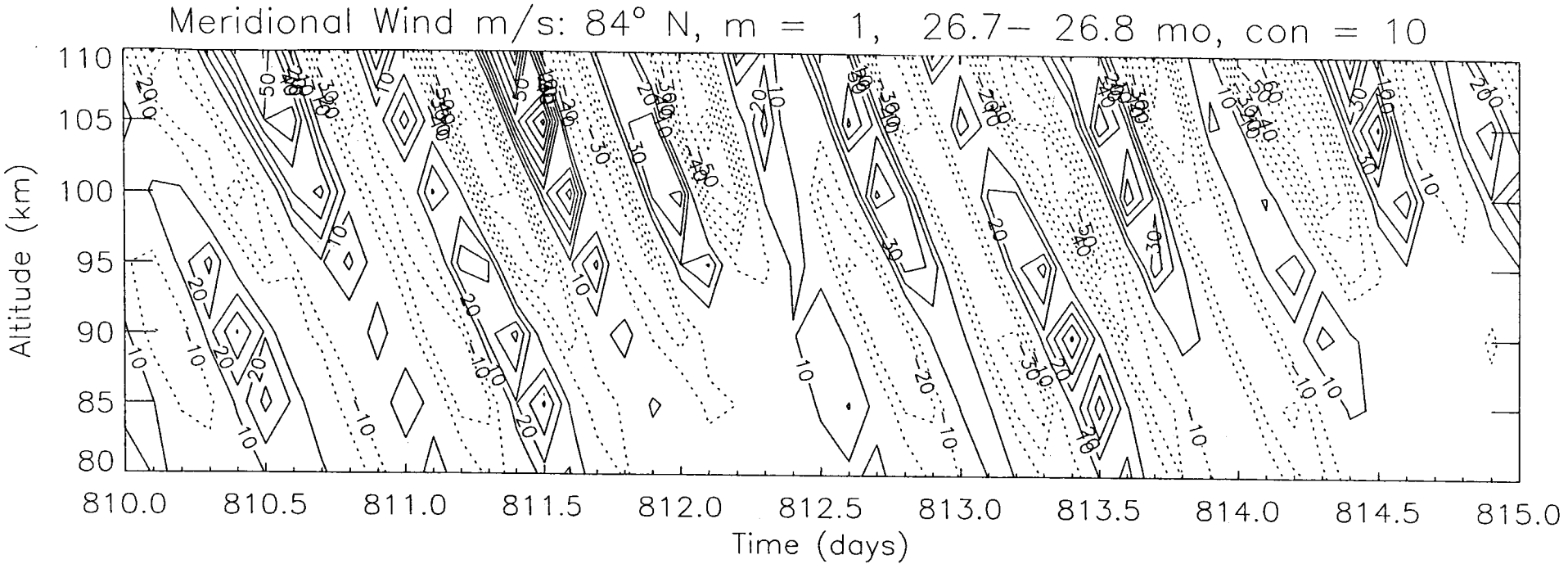

a

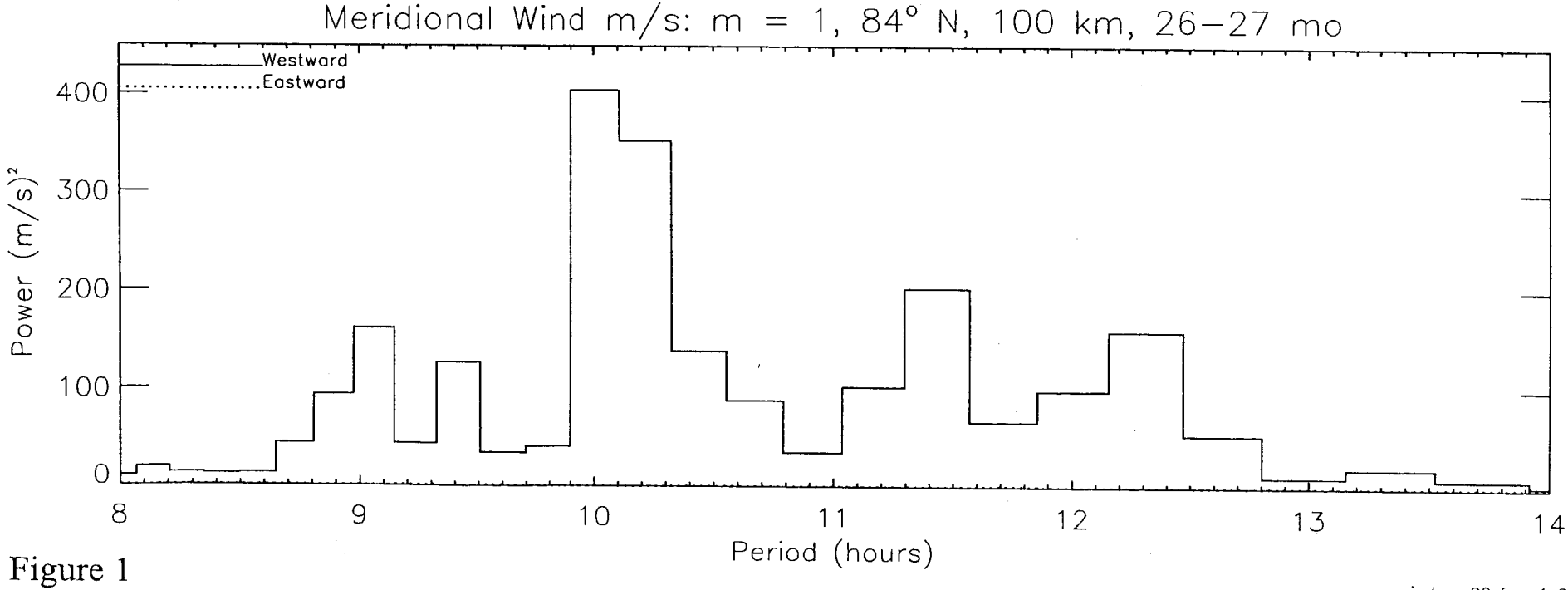

b

Figure 1

window=20 fac=1 C661

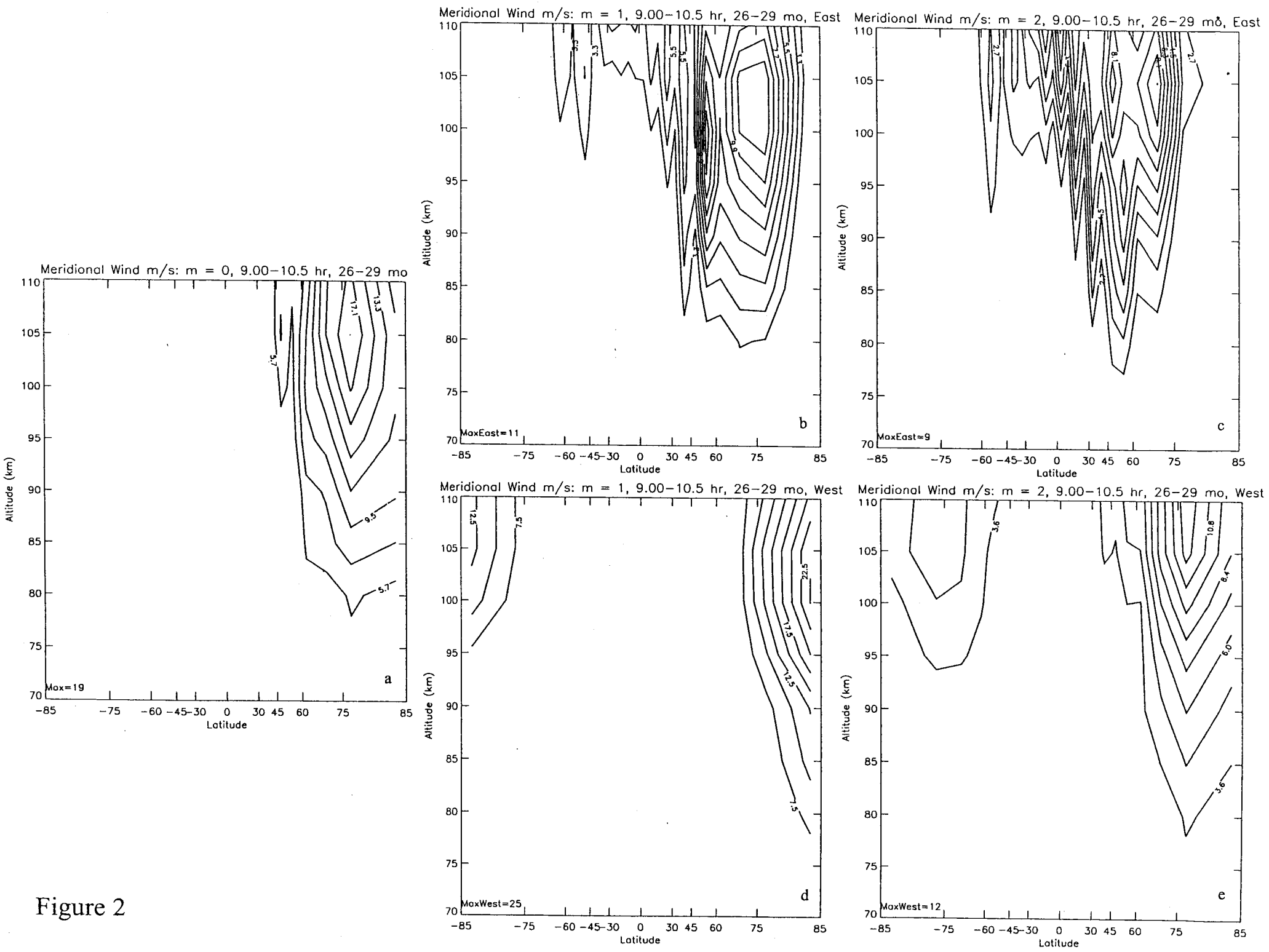
Meridional Wind m/s: m = 0, 9.00–10.5 hr, 26–29 mo
Max=19
a
Meridional Wind m/s: m = 1, 9.00–10.5 hr, 26–29 mo, East
MaxEast=11
b
Meridional Wind m/s: m = 2, 9.00–10.5 hr, 26–29 mo, East
MaxEast=9
c
Meridional Wind m/s: m = 1, 9.00–10.5 hr, 26–29 mo, West
MaxWest=25
d
Meridional Wind m/s: m = 2, 9.00–10.5 hr, 26–29 mo, West
MaxWest=12
e
Altitude (km)
Latitude
110
105
100
95
90
85
80
75
70
-85 -75 -60 -45 -30 0 30 45 60 75 85

Figure 2

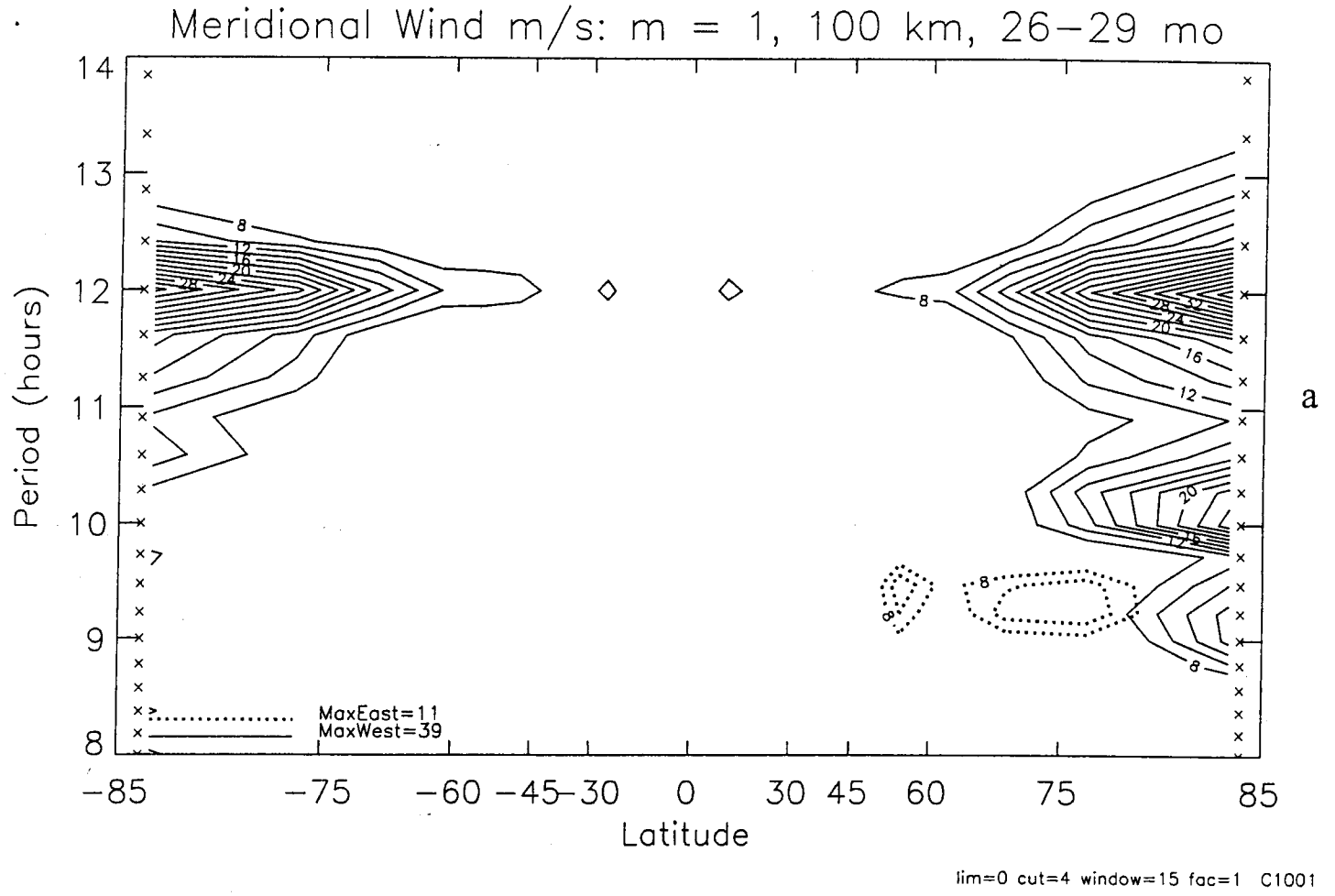
Meridional Wind m/s: m = 1, 100 km, 26–29 mo
Period (hours)
Latitude
MaxEast=11
MaxWest=39
lim=0 cut=4 window=15 fac=1 C1001

a

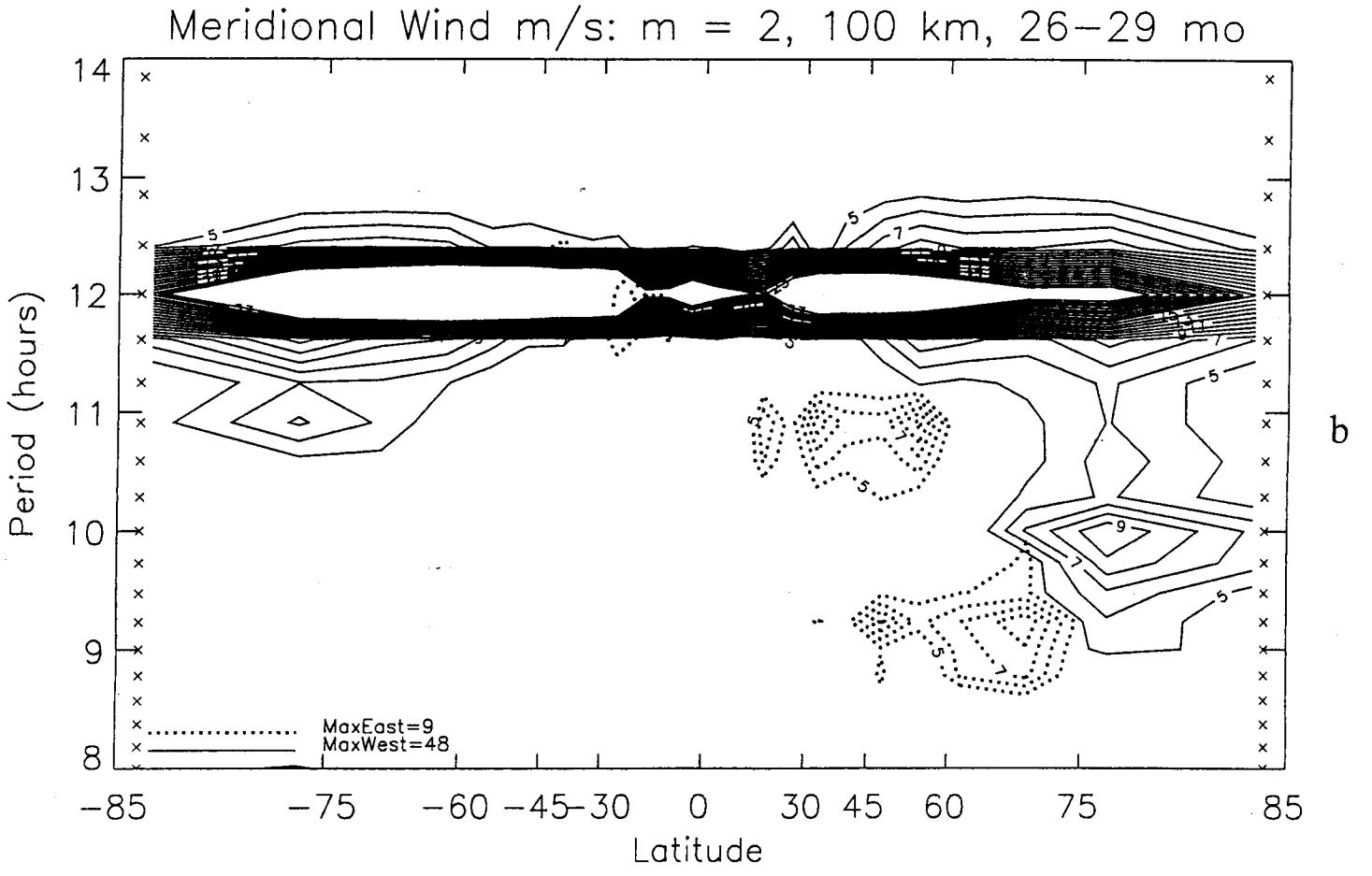
Meridional Wind m/s: m = 2, 100 km, 26–29 mo
Period (hours)
Latitude
MaxEast=9
MaxWest=48
lim=0 cut=5 window=15 fac=1 C1002

b

Figure 3

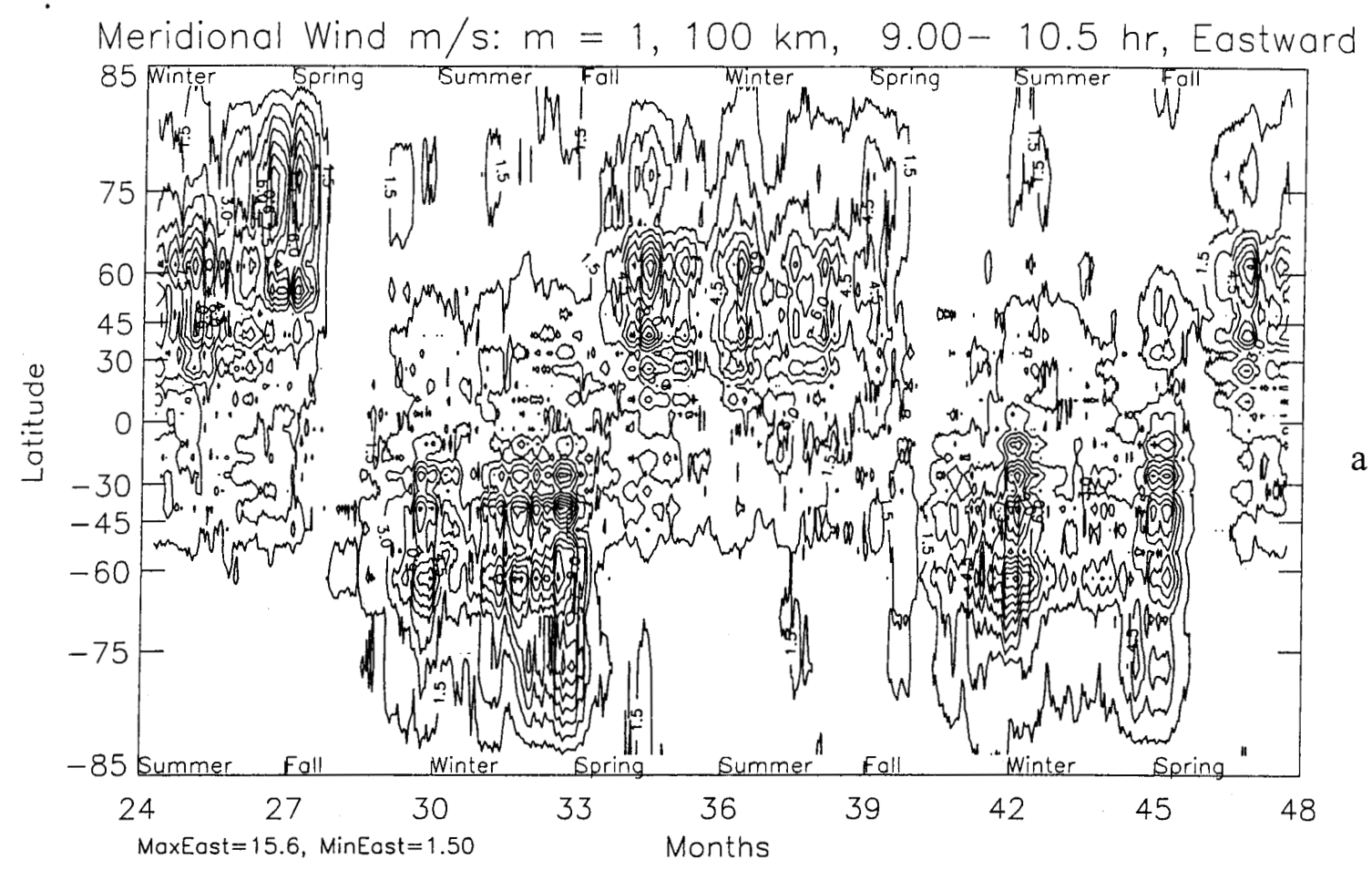
Meridional Wind m/s: m = 1, 100 km, 9.00– 10.5 hr, Eastward
Winter
Spring
Summer
Fall
Winter
Spring
Summer
Fall
85
75
60
45
30
0
−30
−45
−60
−75
−85
Latitude
Summer
Fall
Winter
Spring
Summer
Fall
Winter
Spring
24
27
30
33
36
39
42
45
48
MaxEast=15.6, MinEast=1.50
Months

a

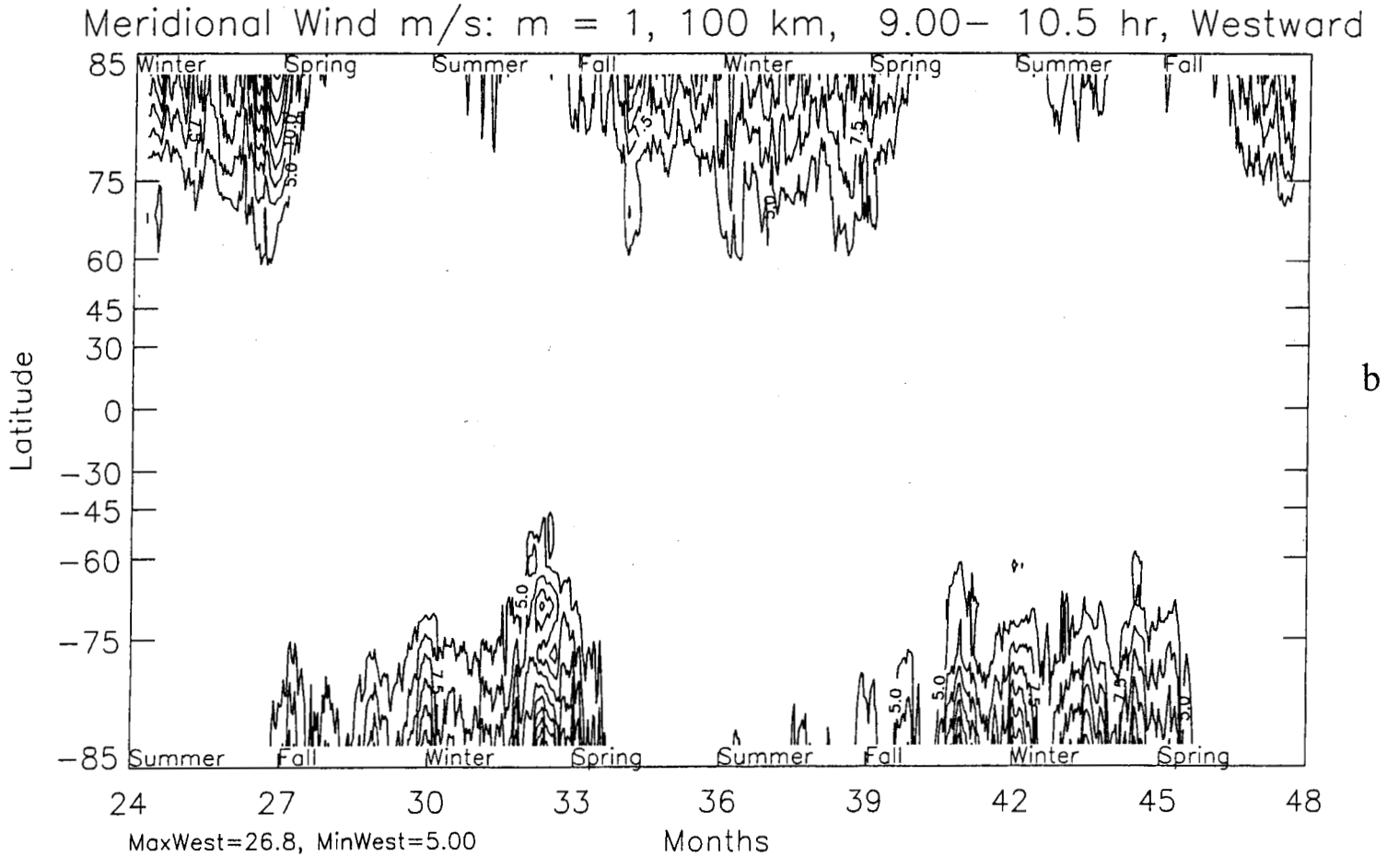
Meridional Wind m/s: m = 1, 100 km, 9.00– 10.5 hr, Westward
Winter
Spring
Summer
Fall
Winter
Spring
Summer
Fall
85
75
60
45
30
0
−30
−45
−60
−75
−85
Latitude
Summer
Fall
Winter
Spring
Summer
Fall
Winter
Spring
24
27
30
33
36
39
42
45
48
MaxWest=26.8, MinWest=5.00
Months
window=15 ndpa,ndpb=40 34 fac=1 C719

b

Figure 4

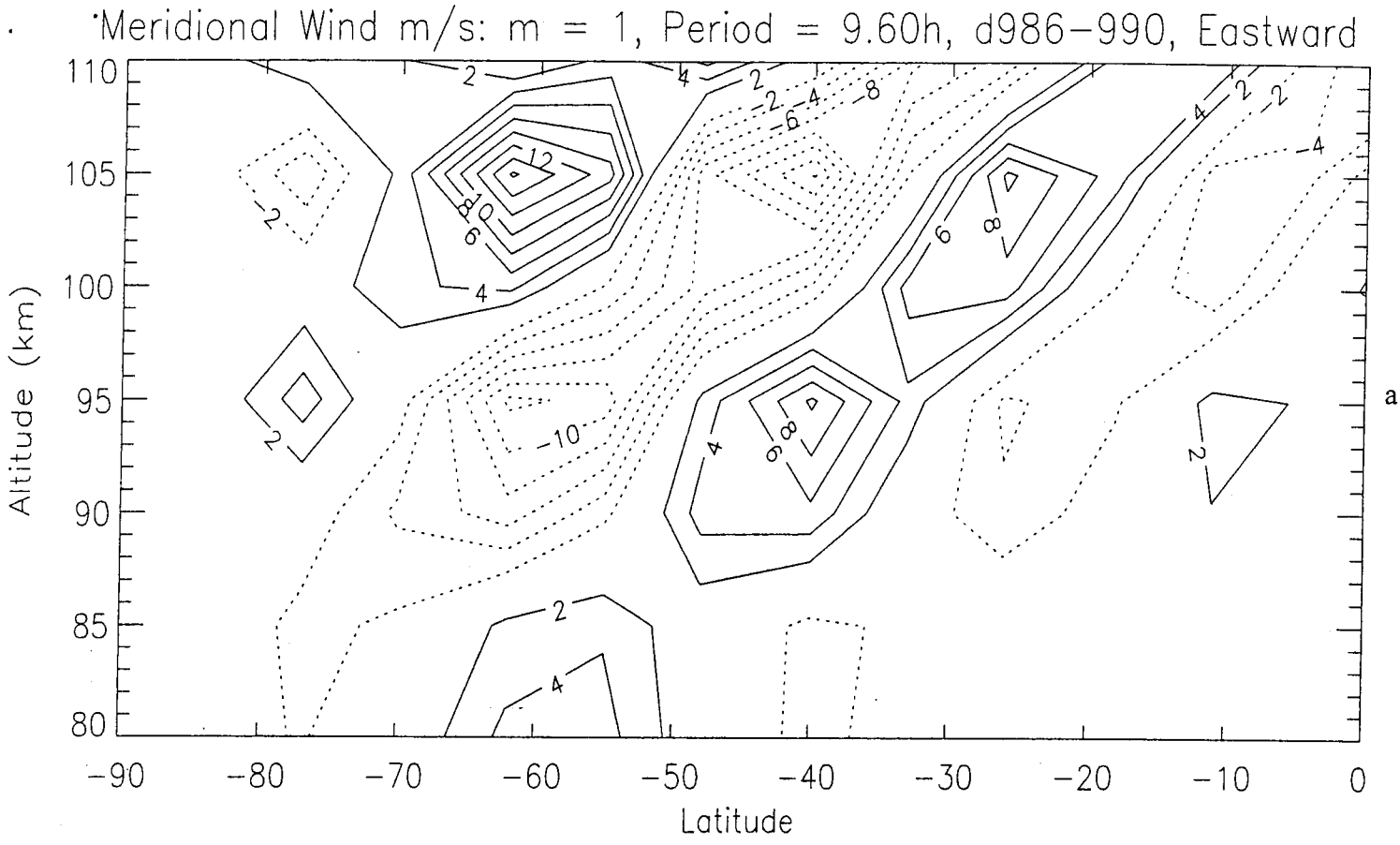
Meridional Wind m/s: m = 1, Period = 9.60h, d986-990, Eastward
Altitude (km)
Latitude
110
105
100
95
90
85
80
-90
-80
-70
-60
-50
-40
-30
-20
-10
0
a

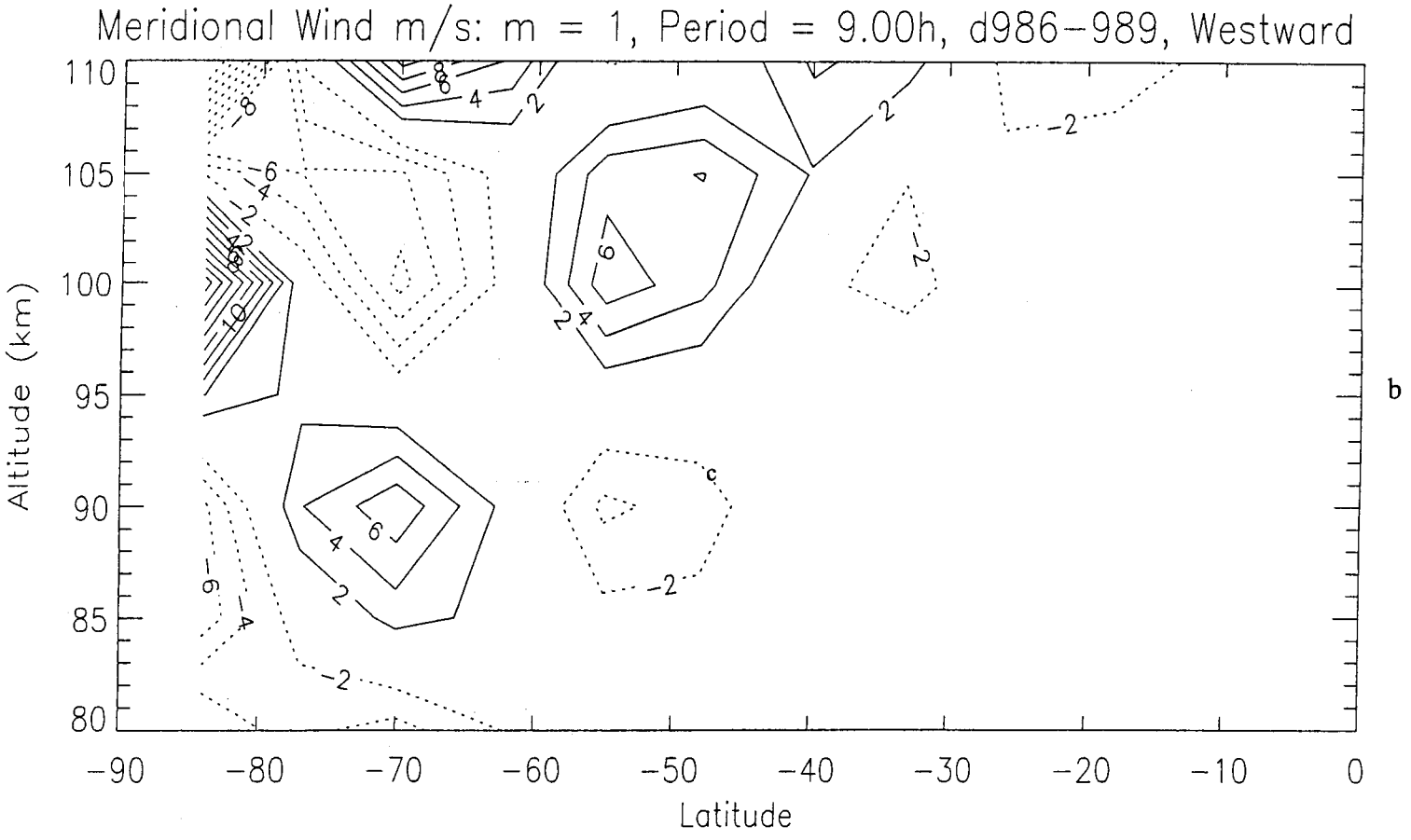
Meridional Wind m/s: m = 1, Period = 9.00h, d986-989, Westward
Altitude (km)
Latitude
110
105
100
95
90
85
80
-90
-80
-70
-60
-50
-40
-30
-20
-10
0
b
c

Figure 5